HHS Public Access

Author manuscript

J Neurochem. Author manuscript; available in PMC 2018 December 01.

Published in final edited form as:

J Neurochem. 2017 December ; 143(6): 635–644. doi:10.1111/jnc.14231.

Impaired AMPA receptor trafficking by a double knockout of zebrafish *olfactomedin1a/b*

Naoki Nakaya, **Afia Sultana**, and **Stanislav I. Tomarev**

Section of Retinal Ganglion Cell Biology, Laboratory of Retinal Cell and Molecular Biology, National Eye Institute, NIH Bethesda, MD 20892

Abstract

The *olfm1a and olfm1b* genes in zebrafish encode conserved secreted glycoproteins. These genes are preferentially expressed in the brain and retina starting from 16 h post-fertilization until adulthood. Functions of the Olfm1 gene is still unclear. Here, we produced and analyzed a null zebrafish mutant of both *olfm1a* and *olfm1b* genes (*olfm1* null). *olfm1* null fish were born at a normal Mendelian ratio and showed normal body shape and fertility as well as no visible defects from larval stages to adult. Olfm1 proteins were preferentially localized in the synaptosomes of the adult brain. Olfm1 co-immunoprecipitated with GluR2 and SNARE complexes indicating participation of Olfm1 in both pre- and post-synaptic events. Phosphorylation of GluR2 was not changed while palmitoylation of GluR2 was decreased in the brain synaptosomal membrane fraction of *olfm1* null compared with wt fish. The levels of GluR2, SNAP25, flotillin1 and VAMP2 were markedly reduced in the synaptic microdomain of *olfm1* null brain compared with wt. The internalization of GluR2 in retinal cells and the localization of VAMP2 in brain synaptosome were modified by *olfm1* null mutation. This indicates that Olfm1 may regulate receptor trafficking from the intracellular compartments to the synaptic membrane microdomain, partly through the alteration of post-translational GluR2 modifications such as palmitoylation. Olfm1 may be considered a novel regulator of the composition and function of the AMPAR complex.

Graphical Abstract

Olfactomedin 1 (Olfm1) is known to interact with the AMPA receptor complex. This study shows that Olfm1 is preferentially localized in the synaptosomes of the adult brain. Olfm1 may regulate receptor trafficking from the intracellular compartments to the synaptic membrane microdomain, partly through the alteration of post-translational GluR2 modifications such as palmitoylation. Olfm1 may be considered a novel regulator of the composition and function of the AMPAR complex.

Address correspondence and reprint request to Stanislav I. Tomarev, PhD., 6 Center Drive, Room 212, Section of Retinal Ganglion Cell Biology, Laboratory of Retinal Cell and Molecular Biology, National Eye Institute, NIH, Bethesda, MD 20892. tomarevs@nei.nih.gov. Tel. 301-496-8524.

DR. NAOKI NAKAYA (Orcid ID : 0000-0003-2200-5200)

conflict of interest disclosure.

The authors have no conflict of interest related to this research.

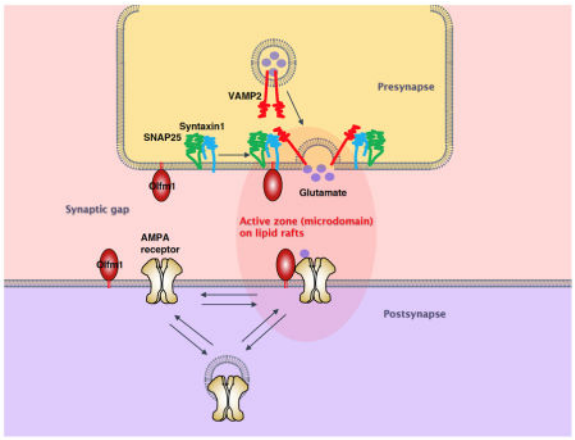

Keywords

Olfactomedin 1; zebrafish; AMPA receptor; lipid raft; palmitoylation

Introduction

Olfactomedin domain-containing proteins form a family consisting of at least 13 members in mammals (Anholt, 2014; Tomarev and Nakaya, 2009). This family can be subdivided into 7 subfamilies on the basis of domain organization, expression patterns, and biochemical properties of individual members (Zeng et al., 2005). Most of the family members are secreted glycoproteins with not-well defined functions. Myocilin, the only member in subfamily III, has been studied more than other family members mainly because mutations in the *MYOCILIN* gene can lead to primary open angle glaucoma, one of the leading causes of blindness (Adam et al., 1997; Stone et al., 1997). The *MYOCILIN* gene is preferentially expressed in non-neuronal tissues showing the highest levels of expression in the trabecular meshwork and sclera of the eye (Adam et al., 1997; Torrado et al., 2002). Olfactomedin 1 (Olfm1), also known as noelin in chicken and *Xenopus*, pancortin in mice, olfactomedin-related glycoprotein in rats, and hOlfA in humans, is a highly conserved secreted glycoprotein that is structurally similar to Olfactomedin 2 (Olfm2) and Olfactomedin 3 (Olfm3) proteins (Tomarev and Nakaya, 2009). These three proteins form subfamily I and are preferentially expressed in neuronal tissues including retina. In most neuronal tissues tested, the level of *Olfm1* gene expression is higher than the levels of *Olfm2* and *Olfm3* expression (Sultana et al., 2011).

Although functions of Olfm1-3 proteins are still poorly understood, available data suggest that Olfm1 plays a role in axon growth in mice (Nakaya et al., 2012), maintenance of neuronal precursor cells in *Xenopus* (Moreno and Bronner-Fraser, 2005), neural crest production in chicken (Barembaum et al., 2000), and optic nerve arborization in the optic tectum in zebrafish (Nakaya et al., 2008). The identification of the protein complexes containing Olfm1 led to several new ideas concerning possible functions of Olfm1-3. In particular, it has been shown that Olfm1-3 are components of the AMPAR complex (Nakaya et al., 2013; Schwenk et al., 2014; Schwenk et al., 2012; Shanks et al., 2012; Sultana et al.,

2014). The AMPAR is the major ionotropic glutamate receptor responsible for the fast excitatory synaptic transmission, postsynaptic plasticity, and synapse development in the central nervous system (Henley and Wilkinson, 2016; Huganir and Nicoll, 2013). More than 30 proteins have been identified in the AMPAR complex (Schwenk et al., 2014; Schwenk et al., 2012; Shanks et al., 2012) and published data demonstrates that its properties and functions depend upon protein composition of the complex (Haering et al., 2014; Straub and Tomita, 2012).

One possible approach to elucidate the functional roles of Olfm1-3 in AMPAR is to produce and analyze null mutants of the corresponding genes. The presumptive *Olfm1* knockout mice actually express a truncated form of Olfm1 with a deletion of 52 amino acids in the central part of the protein molecule (Cheng et al., 2007; Nakaya et al., 2013). Recently, we generated *Olfm2* knockout mice and demonstrated that they were viable and produced at the normal Mendelian ratio. At the same time, *Olfm2* null mice had mildly impaired visual, olfactory, and motor functions and demonstrated reduced levels of several components of the AMPAR complex (Olfm1, PSD95 and CNIH2) in GluR2 immunoprecipitates from the synaptosomal membranes (Sultana et al., 2014). No *Olfm1* complete knockout has been described.

Here, we report the production and characterization of *olfm1* null zebrafish. Zebrafish have 2 *olfm1* genes, *olfm1a* and *olfm1b*, that demonstrate overlapping expression patterns (Nakaya and Tomarev, 2007). We demonstrate that Olfm1 is a lipid raft protein in the brain that interacts not only with AMPAR proteins but also with presynaptic SNARE complex proteins. The knockdown of two *olfm1* genes modified the composition of lipid raft proteins *in vivo* and internalization of GluR2 in neuronal cultures *in vitro.*

Materials and methods

Reagents and antibodies

Antibodies and their working dilutions are listed in Table 1. AMPA and tricaine were purchased from Sigma.

Animals

All animals used in the experiments were managed according to the Association for Research in Vision and Ophthalmology (ARVO) statement for the use of animals in ophthalmic and vision research. All experiments using animals were approved by the NEI Animal Care and Use Committee. Zebrafish were maintained as previously described (Nakaya et al., 2008). *olfm1a*^{sa221} and *olfm1b*^{sa157} were provided by the Welcome Trust Sanger Institute and backcrossed several times with wild-type (wt) TL strain fishes. Adult (6–12 month old) male and female zebrafish were used for this study. For genotyping, genomic DNA was extracted from individual fish tail or larva body trunk using KAPA Express Extract (KAPA biosystems). *Olfm1a* and *b* genomic DNA sequences are available at Genbank (NC_007116 and NC_007132). Target sequences (~600 bp) were amplified by PCR using the following primers and sequenced for each *olfm1a* and *b* point mutations:

olfm1a-FW: 5′-GCATCAACTGGCCAAAAACACTCA-3′

olfm1a-RV: 5′-CCAAAGCGAACTCCCCTCAGAA-3′

olfm1b-FW: 5′-CGGGACCAGACCCTCTCTGTCTAA-3′

olfm1b-RV: 5′-CGCGGAATTGCATCATTGTCTATC-3′

For conventional genotyping, SNP detection assays for these particular point mutations were designed by Invitrogen and used for allele discrimination analysis by quantitative real-time PCR (Q-PCR) (Applied Biosystems). This study was not pre-registered.

Western blotting

Tissues were lysed in the lysis buffer (10 mM Tris-HCl, pH 7.4, 1 mM EDTA, 150 mM NaCl, 1% NP40, 10% glycerol, 5 mM NaF, 0.5 mM sodium orthovanadate, protease inhibitor cocktail (Sigma), halt phosphatase inhibitor cocktail (Thermo Scientific)). The lysed tissues were spun at 14,000 g for 5 min, soluble supernatants were collected and protein concentrations were measured by the BCA assay (Thermo Scientific). The extracted proteins (2 μg) were separated on a 10% SDS-PAGE gel (Invitrogen) and transferred to a PVDF membrane (Invitrogen). The membranes were incubated with a primary antibody followed by incubation with a secondary antibody conjugated to horseradish peroxidase (HRP). The HRP signals were detected using a chemi-luminescence detection kit (SuperSignal Femto Dura Extended Duration Substrate, Pierce) and FluorChem M (Protein Simple). All Western blotting experiments were repeated at least 3 times and protein expression levels were quantitated using Alpha View software (Protein Simple).

Co-Immunoprecipitation

Primary antibodies (10 μg) were cross-linked to protein A/G agarose beads using a crosslink IP kit (Pierce). Fish brain or retina lysates were incubated with primary antibody beads or control rabbit or mouse IgG beads at 4°C overnight. The beads were washed 5 times with a lysis buffer and proteins bound to the beads were eluted with an elution buffer (60 μl) provided with the IP kit. All co-immunoprecipitation experiments were repeated at least 3 times.

Tissue fractionation

Zebrafish whole brain or retina lysates were fractionated as described previously (Hallett et al., 2008). Briefly, for the synaptic membrane fraction, brains were homogenized in an ice cold TEVP buffer (10 mM Tris base, 5 mM NaF, 1mM Na_3VO_4, 1 mM EDTA, 1 mM EGTA, 1x protease inhibitor cocktail, pH 7.4) containing 320 mM sucrose and centrifuged to separate supernatant (S1) and precipitate (P1) fractions for 10 min at 800 g at 4°C. The S1 fraction was further centrifuged for 15 min at 9,200 g at 4°C to separate supernatant (S2) and precipitate (P2) fractions. The crude synaptosomal P2 fraction was re-suspended in TEVP buffer containing 35.6 mM sucrose and then centrifuged for 20 min at 25,000 g at 4°C to separate supernatant (LS1) and precipitate (LP1) containing the synaptosomal membranes. The LS1 fraction was further centrifuged for 1 hr at 65,000 g to isolate the synaptic vesicle LP2 fraction. The S2 fraction was also centrifuged for 1 hr at 65,000 g to isolate the light membrane P3 fraction and cytosolic S3 fraction.

Palmitoylation assay

The palmitoylation of proteins was analyzed as described (Brigidi and Bamji, 2013). The brain LP2 fraction was suspended in the lysis buffer containing 50 mM N-ethylmaleimide (NEM). The lysate was mixed with proteinA/G agarose crosslinked with anti-Olfm1 or anti-GluR2 antibody as described above overnight at 4°C. After washing, the beads were resuspended in lysis buffer (pH7.2) and treated or untreated with 1M hydroxylamine (HAM) for 1 hr at room temperature. The beads were again washed and free thiol residues were crosslinked with BSS-biotin in lysis buffer (pH6.2) for 1 hr at 4°C. The beads were finally washed with lysis buffer three times and all proteins were eluted with elution buffer (pH2.8). Biotin-crosslinked proteins were separated on an 10% SDS-PAGE gel and detected with horse radish peroxidase (HRP)-conjugated streptoavidin.

Internalization assay

Eyes were dissected from 32 hpf embryos. A lens was removed from each dissected eye, remaining retina was divided into 4–5 fragments, and retinal fragments were cultured in culture medium (Leibovitz's L15 with 10% fetal bovine serum and penicillin/streptomycin:water =70:30) for 5 days at 28°C. Internalization assay of GluR2 was performed as described (Lin et al., 2000). The external GluR2 was labeled with the medium containing anti-GluR2 monoclonal antibody (5 mg/ml) for 15 min at 28°C. After washing with the growth medium, cultures were incubated in the presence or absence of 100 mM AMPA for 15 min at 28°C to allow the internalization of labeled receptors. Cells were fixed with 4% PFA/4% sucrose in PBS for 5 min and washed and blocked with PBS -1% BSA for 1 hr. The external GluR2 receptors were labeled with Alexa 488-anti-mouse IgG in PBS-1% BSA for 1 hr at room temperature. After washing with PBS-0.05% Tween20, the incorporated GluR2 receptors were labeled with Alexa 555-anti mouse IgG in PBS-0.05% Tween20-1% BSA. After washing with PBS-0.05% Tween20, images were analyzed using Zeiss LSM 700 confocal microscope. The ratio of surface and internalized GluR2 receptors was quantitated by counting the number of green and red puncta in cells using Image J software.

Isolation of brain microdomain

Isolation of microdomain from adult zebrafish brain was performed as described (Maekawa et. al., 1999). Tissues were homogenized in TME buffer (10 mM Tris-HCl, 1 mM MgCl2 and 1 mM EGTA, pH7.5) with 2% Triton X-100 and spun once at 900 g for 10 min to remove debris. Sucrose was added to the homogenates up to 0.8 M and the homogenates were placed at the bottom of a centrifuge tube. TME with and without 0.7 M sucrose were gently overlaid sequentially to form discontinuous sucrose gradient. The tube was spun at 70,000 x g for 6 hr. The lipid raft band between the top two layers was collected and precipitated by a centrifugation at 100,000 x g for 1 hr.

Statistical analysis

Data were analyzed using the unpaired Student's t test preceded by F test for variances or one way ANOVA test.

Results

Generation of zebrafish *olfm1a* and *olfm1b* double knockout

The *olfm1a*^{sa221} mutant contained a stop codon at position Gln39 and Gln67 in AMZ/AMY and BMZ/BMY forms, respectively. For the *olfm1b*^{sa157} mutant, a stop codon was located at position Gln33 and Gln61 in AMZ/AMY and BMZ/BMY forms, respectively (Fig. 1a, b). The first 26 and 16 amino acids in the AMZ/AMY and BMZ/BMY forms of olfm1a and olfm1b proteins, respectively, correspond to the signal peptides. Only short protein fragments with a length of 12, 50, 6 and 44 amino acids could be produced after cleavage of the signal peptide in *olfm1a* AMZ/AMY, *olfm1a* BMZ/BMY, *olfm1b* AMZ/AMY, and *olfm1b* BMZ/BMY forms, respectively, suggesting that *olfm1a*^{sa221} and *olfm1b*^{sa157} mutants are the null mutants of the corresponding genes. They were crossbred to generate double null mutants of the *olfm1a* and *olfm1b* genes (*olfm1* null). High throughput RNAseq revealed the presence of mRNAs encoding *olfm1a* and *olfm1b* in *olfm1* mutants at reduced levels (40.7% of *olfm1a* mRNA and 65.4% of *olfm1b* mRNA relatively to those in wt samples; Nakaya and Tomarev, in preparation), however neither olfm1a nor olfm1b proteins were detected in mutants by Western blot analysis, confirming that these alleles are null mutations (Fig. 1c). *olfm1* null fish were born at a normal Mendelian ratio and showed normal body shape and fertility as well as no visible defects from larval stages to adult.

Elimination of olfm1 produces changes in presynaptic SNARE and postsynaptic AMPAR complexes

Previous studies in mice demonstrated that Olfm1 may interact with several pre- and postsynaptic proteins including components of the AMPAR complex, teneurin-4, kidins220, Cav2.1, and synaptophysin (Nakaya et al., 2013; Schwenk et al., 2014; Schwenk et al., 2012; Shanks et al., 2012). To test whether olfm1 absence may affect the level of some presynaptic SNARE complex proteins and postsynaptic proteins, we compared their levels in adult brain and retina of *olfm1* null and wt fish by Western blotting (Fig. 2a). Changes in the levels of tested proteins were not dramatic (if any) in both brain and retina samples and only synaptophysin and VAMP showed statistically significant elevation in the brain samples of *olfm1* null compared with wt fish (Fig. 2b). To analyze the intracellular distribution of Olfm1 in neuronal tissues, we used zebrafish adult brain since the amount of retinal tissues was limited. The brain homogenates were separated into different membrane and soluble fractions and these fractions were analyzed by Western blotting. The Olfm1 protein was preferentially detected in the synaptosomal membrane LP1 fraction. It was also detected in other membrane (P3) and insoluble (P1) fractions, while soluble (S3) or synaptic vesicle fractions (LP2) did not contain detectable amounts of Olfm1 (Fig. 2c). The presence of Olfm1 in the P1 fraction containing cell debris reflects the fact that a portion of Olfm1 could be present in an insoluble form. As expected, several tested synaptic proteins including GluR2 were also detected in the LP1 fraction, while presynaptic vesicle proteins, VAMP2 and synaptophysin, were more abundant in the LP2 fraction than in other fractions.

To test whether Olfm1 forms a complex with tested synaptic and SNARE proteins, we used the LP1 fraction from wt and *olfm1* null brains for immunoprecipitation using antibodies against VAMP2 and syntaxin1 (Fig. 2e, f). Olfm1 was co-immunoprecipitated with both

Vamp2 and syntaxin1. Since Olfm1 was not detected in the LP2 and S3 fractions (Fig. 2c), co-immunoprecipitation of Olfm1 with synaptic and SNARE proteins indicates that it is associated with the synaptosomal membrane. The amounts of VAMP2 co-immunoprecipitated with syntaxin1 and the amount of syntaxin1 co-immunoprecipitated with VAMP2 were similar in wt and *olfm1* null synaptosomal membranes (Fig. 2e, f). This is in line with an observation that an increase in the VAMP2 level occurs in the synaptic vesicles of *olfm1* null compared with wt samples (Fig. 2a, b).

Olfm1 null mutation leads to reduced internalization of GluR2 and accumulation of VAMP2 in synaptic vesicle pool

Next, we analyzed the distribution of GluR2 in *olfm1* null synaptosomal membranes. GluR2 was co-immunoprecipitated with Olfm1 from the synaptosomal fraction of wt zebrafish as it has been previously observed in a mouse brain (Fig. 2d). Although the functional role of Olfm1 in the AMPAR complex is not understood yet, we hypothesize that Olfm1 might be involved in the regulation of GluR2 membrane trafficking. To determine whether trafficking of GluR2 was affected in *olfm1* null zebrafish, we utilized the internalization assay using zebrafish retinal explant cultures. Retinas dissected from 32 hpf wt and *olfm1* null larvae were cultivated for 5 days and then internalization of GluR2 receptors with or without AMPA treatment (100 mM for 15 min) was analyzed as described in Materials and Methods. Counting of the surface (green puncta) and internalized (red puncta) GluR2 receptors demonstrated that the internalization of GluR2 in *olfm1* null samples was reduced compared with control samples both in the absence and presence of AMPA, but the reduction was more pronounced in the latter case (Fig. 3a, b). Phosphorylation of GluR2 at Tyr 869, 873 and 876 was similar between wt and *olfm1* null samples (Fig. 3c). At the same time, the palmitoylation of GluR2 was greatly reduced in *olfm1* null samples compared with wt (Fig. 3d, upper panel). Olfm1 co-precipitated with GluR2 was also palmitoylated, implying that the palmitoylation may mediate the synaptic membrane localization of olfm1 (Fig. 3d, lower panel). This observation indicates that *olfm1* null mutation affects membrane localization of GluR2.

In addition, to investigate whether the membrane localization of presynaptic vesicle proteins affected in *olfm1* null brain, we have analyzed VAMP2 localization in LP1 and LP2 membrane fractions (Fig. 3e, f) The level of VAMP2 was increased in the LP2 fraction of *olfm1* null brain compared with the LP2 fraction of wt brain. There was no difference in the VAMP2 levels in the LP1 fraction (Fig. 3e, f). This suggests either an inhibition in the synaptic vesicle release or acceleration in the internalization of synaptic vesicle in the presynaptic *olfm1* null compartment.

Olfm1 null mutation affects to synaptic microdomain formation

The association of endogenous Olfm1 with brain synaptic membranes, interaction with synaptic membrane proteins, and palmitoylation of olfm1 indicate that Olfm1 may mediate localization of interacting proteins in the synaptic membrane microdomain and affect its composition. To test this hypothesis, we isolated a zebrafish brain microdomain fraction and examined the level of several proteins co-immunoprecipitated with GluR2 from the LP1 fraction as well as flotillin1, a microdomain scaffolding protein (Bodin et al., 2014). The

levels of all tested proteins (GluR2, SNAP25, Flotillin1 and VAMP2) were significantly reduced in the microdomain fraction isolated from *olfm1* null brain compared with wt samples (Fig. 4a, b). In the retina, the IPL was co-stained with anti-GluR2 antibody and a cholera toxin B subunit for lipid rafts to assess the localization of GluR2. In the IPL of wt fish, most GluR2 positive puncta were detected in the lipid rafts, while in *olfm1* null IPL, many such GluR2 puncta were not localized in the rafts (Fig. 4c–e). These findings indicate that GluR2 in/out cycle or the lateral trafficking in the postsynaptic membrane could be altered in the absence of Olfm1.

Discussion

Olfm1 is a highly conserved secreted glycoprotein that is preferentially expressed in neuronal tissues and whose detailed molecular mechanisms are still unclear. Here we describe *olfm1* null zebrafish as a new tool to study functions of Olfm1. There are two *olfm1* genes in zebrafish and null mutations were introduced in both of them. Several knockout mouse lines for genes encoding olfactomedin domain-containing proteins have been reported and include *Myocilin* (Kim et al., 2001), *Olfm2* (Sultana et al., 2014), *Olfml3* (Ikeya et al., 2005), *Olfm4* (Liu et al., 2010) and *Lphn3* (Wallis et al., 2012). All these reported knockout mouse lines were viable and did not show gross abnormalities while a more detailed analysis of their phenotypes revealed a variety of morphological and behavioral defects.

Similar to the above mentioned null mutants in mice, the zebrafish *olfm1* null mutant is viable and did not demonstrate overt abnormalities although minor structural and functional defects were detected in the retina (Nakaya and Tomarev, unpublished). To get insight into possible functions of Olfm1, we looked at the proteins interacting with Olfm1. It has been shown in many cases that interacting proteins or proteins forming a multiprotein complex very often are involved in the same biological processes in normal and pathological states (Barabasi et al., 2011; Ideker and Sharan, 2008; Oti et al., 2006). Several candidate proteins interacting with Olfm1 have been identified by different laboratories using different approaches and include Olfm2, Olfm3 (Nakaya et al., 2013; Sultana et al., 2011), β-dystrobrevin (Veroni et al., 2007), Wif1 (Nakaya et al., 2008), Wave1, and Bcl-xL (Cheng et al., 2007), amyloid precursor protein (Rice et al., 2012), and Nogo-A receptor (Nakaya et al., 2012). Interaction of Olfm1 with AMPAR has been reported by at least three groups (Nakaya et al., 2013; Schwenk et al., 2014; Schwenk et al., 2012; Shanks et al., 2012) although details of this interaction have not been investigated yet. We have previously shown that expression of mutated Olfm1 with a deletion of 52 amino acids in the central part of the protein molecule modifies interaction of Olfm1 with ligand-binding subunits of AMPAR, GluR2 and GluR4, and caused the reduction of brain volume and size of major axon bundles as well as abnormal behavior and olfactory activity (Nakaya et al., 2013).

Expression patterns of zebrafish *olfm1* and *gria1-4* genes encoding GluR1-4 subunits of AMPAR overlap in both retina and brain (Hoppmann et al., 2008; Nakaya and Tomarev, 2007) and are very similar to the expression patterns of corresponding genes in mammals (Dijk and Kamphuis, 2004; Liu et al., 2008; Nakaya et al., 2012). Changes in the composition of AMPARs and trafficking of their subunits may lead to changes in synaptic

transmission in the retina (Casimiro et al., 2013; Henley and Wilkinson, 2016) and changes in escape responses (smaller tail velocities and aberrant turning directions) (Roy et al., 2016). It has been demonstrated that AMPARs mediate synaptic transmission from cone photoreceptors to OFF bipolar cells in zebrafish (Wong et al., 2004). Among AMPAR core subunits, GluR2 has attracted more attention in the literature because of its pronounced effects on AMPAR trafficking and regulation of Ca^{2+} permeability. Moreover, defective control of GluR2 incorporation into AMPAR was linked to neuronal pathologies (Henley and Wilkinson, 2016). The most dramatic changes in the GluR2 level between *olfm1* null and wt fish were observed in the microdomain fraction which share many raft properties. The level of GluR2 was reduced together with the levels of flotilin 1, a marker of microdomains and lipid raft. Basal internalization of AMPARs was increased in raft-depleted neurons (Hering et al., 2003; Hou et al., 2008). It was suggested that raft depletion may disrupt the subcellular targeting of a protein such as palmitoylated GRIP and PSD95, impairing the interaction of these proteins with GluR2 and leading to destabilization of AMPARs at the postsynaptic membrane (DeSouza et al., 2002). Olfm1 co-immunoprecipitated with GluR2 is palmitoylated and may play a role in a stabilization of GluR2 on the membrane. The reduced palmitoylation of GluR2 in *olfm1* null compared with wt fish also may contribute to the reduced level of GluR2 in the microdomain fraction. Exocytotic components such as syntaxin-1, SNAP25 and VAMP2 are associated with lipid rafts (Chamberlain et al., 2001) and our data shows a reduction in their microdomain levels after depletion of Olfm1 leading to reduced internalization of GluR2 compared with wt fish.

The C-terminal domain of Glur1-4 is considered to be a platform for protein interactions essential for AMPAR trafficking and our data identify olfm1 as a novel player in this process. Moreover, available data suggest that Olfm1 is a component of the outer core of the AMPAR complex interacting with the N-terminal domain of GluR2 (Schwenk et al., 2012). Our data support an idea that expanding the range of AMPAR-interacting proteins and elucidation of their detailed roles “will provide a molecular basis for the extraordinary flexibility of neurons to adapt synaptic transmission in response to activity” (Henley and Wilkinson, 2016).

Acknowledgments

This work was supported by the Intramural Research Programs of the National Eye Institute, National Institutes of Health. We thank Welcome Trust Sanger Institute for providing single null *olfm1a* and *olfm1b* zebrafish mutants and Dr. Kawakami for providing a Tol2 plasmid. We thank Dr. Ben Mead for critical reading of the manuscript.

Abbreviations used

AMPAR	AMPA receptor
HAM	hydroxylamine
Olfm1	Olfactomedin 1
SNARE	soluble NSF attachment protein receptor

References

Adam MF, Belmouden A, Binisti P, Brezin AP, Valtot F, Bechetoille A, Dascotte JC, Copin B, Gomez L, Chaventre A, et al. Recurrent mutations in a single exon encoding the evolutionarily conserved olfactomedin-homology domain of TIGR in familial open-angle glaucoma. Hum Mol Genet. 1997; 6:2091–2097. [PubMed: 9328473]

Anholt RR. Olfactomedin proteins: central players in development and disease. Front Cell Dev Biol. 2014; 2:6. [PubMed: 25364714]

Barabasi AL, Gulbahce N, Loscalzo J. Network medicine: a network-based approach to human disease. Nat Rev Genet. 2011; 12:56–68. [PubMed: 21164525]

Barembaum M, Moreno TA, LaBonne C, Sechrist J, Bronner-Fraser M. Noelin-1 is a secreted glycoprotein involved in generation of the neural crest. Nat Cell Biol. 2000; 2:219–225. [PubMed: 10783240]

Bodin S, Planchon D, Rios Morris E, Comunale F, Gauthier-Rouviere C. Flotillins in intercellular adhesion - from cellular physiology to human diseases. J Cell Sci. 2014; 127:5139–5147. [PubMed: 25413346]

Brigidi GS, Bamji SX. Detection of protein palmitoylation in cultured hippocampal neurons by immunoprecipitation and acyl-biotin exchange (ABE). J Vis Exp. 2013; 18:72.

Casimiro TM, Nawy S, Carroll RC. Molecular mechanisms underlying activity-dependent AMPA receptor cycling in retinal ganglion cells. Mol Cell Neurosci. 2013; 56:384–392. [PubMed: 23911793]

Cheng A, Arumugam TV, Liu D, Khatri RG, Mustafa K, Kwak S, Ling HP, Gonzales C, Xin O, Jo DG, et al. Pancortin-2 interacts with WAVE1 and Bcl-xL in a mitochondria-associated protein complex that mediates ischemic neuronal death. J Neurosci. 2007; 27:1519–1528. [PubMed: 17301160]

DeSouza S, Fu J, States BA, Ziff EB. Differential palmitoylation directs the AMPA receptor-binding protein ABP to spines or to intracellular clusters. J Neurosci. 2002; 22:3493–3503. [PubMed: 11978826]

Dijk F, Kamphuis W. Ischemia-induced alterations of AMPA-type glutamate receptor subunit. Expression patterns in the rat retina - an immunocytochemical study. Brain Res. 2004; 997:207–221. [PubMed: 14706873]

Haering SC, Tapken D, Pahl S, Hollmann M. Auxiliary subunits: shepherding AMPA receptors to the plasma membrane. Membranes. 2014; 4:469–490. [PubMed: 25110960]

Hallett PJ, Collins TL, Standaert DG, Dunah AW. Biochemical fractionation of brain tissue for studies of receptor distribution and trafficking. Curr Protocols Neurosci. 2008; 42:1.16.16.

Henley JM, Wilkinson KA. Synaptic AMPA receptor composition in development, plasticity and disease. Nat Rev. 2016; 17:337–350.

Hering H, Lin CC, Sheng M. Lipid rafts in the maintenance of synapses, dendritic spines, and surface AMPA receptor stability. J Neurosci. 2003; 23:3262–3271. [PubMed: 12716933]

Hoppmann V, Wu JJ, Soviknes AM, Helvik JV, Becker TS. Expression of the eight AMPA receptor subunit genes in the developing central nervous system and sensory organs of zebrafish. Dev Dyn. 2008; 237:788–799. [PubMed: 18224707]

Hou Q, Huang Y, Amato S, Snyder SH, Huganir RL, Man HY. Regulation of AMPA receptor localization in lipid rafts. Mol Cell Neurosci. 2008; 38:213–223. [PubMed: 18411055]

Huganir RL, Nicoll RA. AMPARs and synaptic plasticity: the last 25 years. Neuron. 2013; 80:704–717. [PubMed: 24183021]

Ideker T, Sharan R. Protein networks in disease. Genome Res. 2008; 18:644–652. [PubMed: 18381899]

Ikeya M, Kawada M, Nakazawa Y, Sakuragi M, Sasai N, Ueno M, Kiyonari H, Nakao K, Sasai Y. Gene disruption/knock-in analysis of mONT3: vector construction by employing both in vivo and in vitro recombinations. Int J Dev Biol. 2005; 49:807–823. [PubMed: 16172977]

Kim BS, Savinova OV, Reedy MV, Martin J, Lun Y, Gan L, Smith RS, Tomarev SI, John SW, Johnson RL. Targeted disruption of the Myocilin Gene (Myoc) suggests that human glaucoma-causing mutations are gain of function. Mol Cell Biol. 2001; 21:7707–7713. [PubMed: 11604506]

Liu P, Smith PF, Darlington CL. Glutamate receptor subunits expression in memory-associated brain structures: regional variations and effects of aging. Synapse. 2008; 62:834–841. [PubMed: 18720514]

Liu W, Yan M, Liu Y, Wang R, Li C, Deng C, Singh A, Coleman WG Jr, Rodgers GP. Olfactomedin 4 down-regulates innate immunity against Helicobacter pylori infection. Proc Natl Acad Sci U S A. 2010; 107:11056–11061. [PubMed: 20534456]

Moreno TA, Bronner-Fraser M. Noelins modulate the timing of neuronal differentiation during development. Dev Biol. 2005; 288:434–447. [PubMed: 16289448]

Nakaya N, Lee HS, Takada Y, Tzchori I, Tomarev SI. Zebrafish olfactomedin 1 regulates retinal axon elongation in vivo and is a modulator of Wnt signaling pathway. J Neurosci. 2008; 28:7900–7910. [PubMed: 18667622]

Nakaya N, Sultana A, Lee HS, Tomarev SI. Olfactomedin 1 interacts with the nogo a receptor complex to regulate axon growth. J Biol Chem. 2012; 287:37171–37184. [PubMed: 22923615]

Nakaya N, Sultana A, Munasinghe J, Cheng A, Mattson MP, Tomarev SI. Deletion in the N-terminal half of olfactomedin 1 modifies its interaction with synaptic proteins and causes brain dystrophy and abnormal behavior in mice. Exp Neurol. 2013; 250:205–218. [PubMed: 24095980]

Nakaya N, Tomarev S. Expression patterns of alternative transcripts of the zebrafish olfactomedin 1 genes. Gene Expr Patterns. 2007; 7:723–729. [PubMed: 17681890]

Oti M, Snel B, Huynen MA, Brunner HG. Predicting disease genes using protein-protein interactions. J Med Genet. 2006; 43:691–698. [PubMed: 16611749]

Rice HC, Townsend M, Bai J, Suth S, Cavanaugh W, Selkoe DJ, Young-Pearse TL. Pancortins interact with amyloid precursor protein and modulate cortical cell migration. Development. 2012; 139:3986–3996. [PubMed: 22992957]

Roy B, Ahmed KT, Cunningham ME, Ferdous J, Mukherjee R, Zheng W, Chen XZ, Ali DW. Zebrafish TARP Cacng2 is required for the expression and normal development of AMPA receptors at excitatory synapses. Dev Neurobiol. 2016; 76:487–506. [PubMed: 26178704]

Schwenk J, Baehrens D, Haupt A, Bildl W, Boudkkazi S, Roeper J, Fakler B, Schulte U. Regional diversity and developmental dynamics of the AMPA-receptor proteome in the mammalian brain. Neuron. 2014; 84:41–54. [PubMed: 25242221]

Schwenk J, Harmel N, Brechet A, Zolles G, Berkefeld H, Muller CS, Bildl W, Baehrens D, Huber B, Kulik A, et al. High-resolution proteomics unravel architecture and molecular diversity of native AMPA receptor complexes. Neuron. 2012; 74:621–633. [PubMed: 22632720]

Shanks NF, Savas JN, Maruo T, Cais O, Hirao A, Oe S, Ghosh A, Noda Y, Greger IH, Yates JR 3rd, et al. Differences in AMPA and kainate receptor interactomes facilitate identification of AMPA receptor auxiliary subunit GSG1L. Cell Rep. 2012; 1:590–598. [PubMed: 22813734]

Stone EM, Fingert JH, Alward WL, Nguyen TD, Polansky JR, Sunden SL, Nishimura D, Clark AF, Nystuen A, Nichols BE, et al. Identification of a gene that causes primary open angle glaucoma. Science. 1997; 275:668–670. [PubMed: 9005853]

Straub C, Tomita S. The regulation of glutamate receptor trafficking and function by TARPs and other transmembrane auxiliary subunits. Curr Opin Neurobiol. 2012; 22:488–495. [PubMed: 21993243]

Sultana A, Nakaya N, Dong L, Abu-Asab M, Qian H, Tomarev SI. Deletion of olfactomedin 2 induces changes in the AMPA receptor complex and impairs visual, olfactory, and motor functions in mice. Exp Neurol. 2014; 261:802–811. [PubMed: 25218043]

Sultana A, Nakaya N, Senatorov VV, Tomarev SI. Olfactomedin 2: expression in the eye and interaction with other olfactomedin domain-containing proteins. Invest Ophthalmol Vis Sci. 2011; 52:2584–2592. [PubMed: 21228389]

Tomarev SI, Nakaya N. Olfactomedin domain-containing proteins: possible mechanisms of action and functions in normal development and pathology. Mol Neurobiol. 2009; 40:122–138. [PubMed: 19554483]

Torrado M, Trivedi R, Zinovieva R, Karavanova I, Tomarev SI. Optimedin: a novel olfactomedin-related protein that interacts with myocilin. Hum Mol Genet. 2002; 11:1291–1301. [PubMed: 12019210]

Veroni C, Grasso M, Macchia G, Ramoni C, Ceccarini M, Petrucci TC, Macioce P. Beta-dystrobrevin, a kinesin-binding receptor, interacts with the extracellular matrix components pancortins. J Neurosci Res. 2007; 85:2631–2639. [PubMed: 17265465]

Wallis D, Hill DS, Mendez IA, Abbott LC, Finnell RH, Wellman PJ, Setlow B. Initial characterization of mice null for Lphn3, a gene implicated in ADHD and addiction. Brain Res. 2012; 1463:85–92. [PubMed: 22575564]

Wong KY, Gray J, Hayward CJ, Adolph AR, Dowling JE. Glutamatergic mechanisms in the outer retina of larval zebrafish: analysis of electroretinogram b- and d-waves using a novel preparation. Zebrafish. 2004; 1:121–131. [PubMed: 18248224]

Zeng LC, Han ZG, Ma WJ. Elucidation of subfamily segregation and intramolecular coevolution of the olfactomedin-like proteins by comprehensive phylogenetic analysis and gene expression pattern assessment. FEBS Lett. 2005; 579:5443–5453. [PubMed: 16212957]

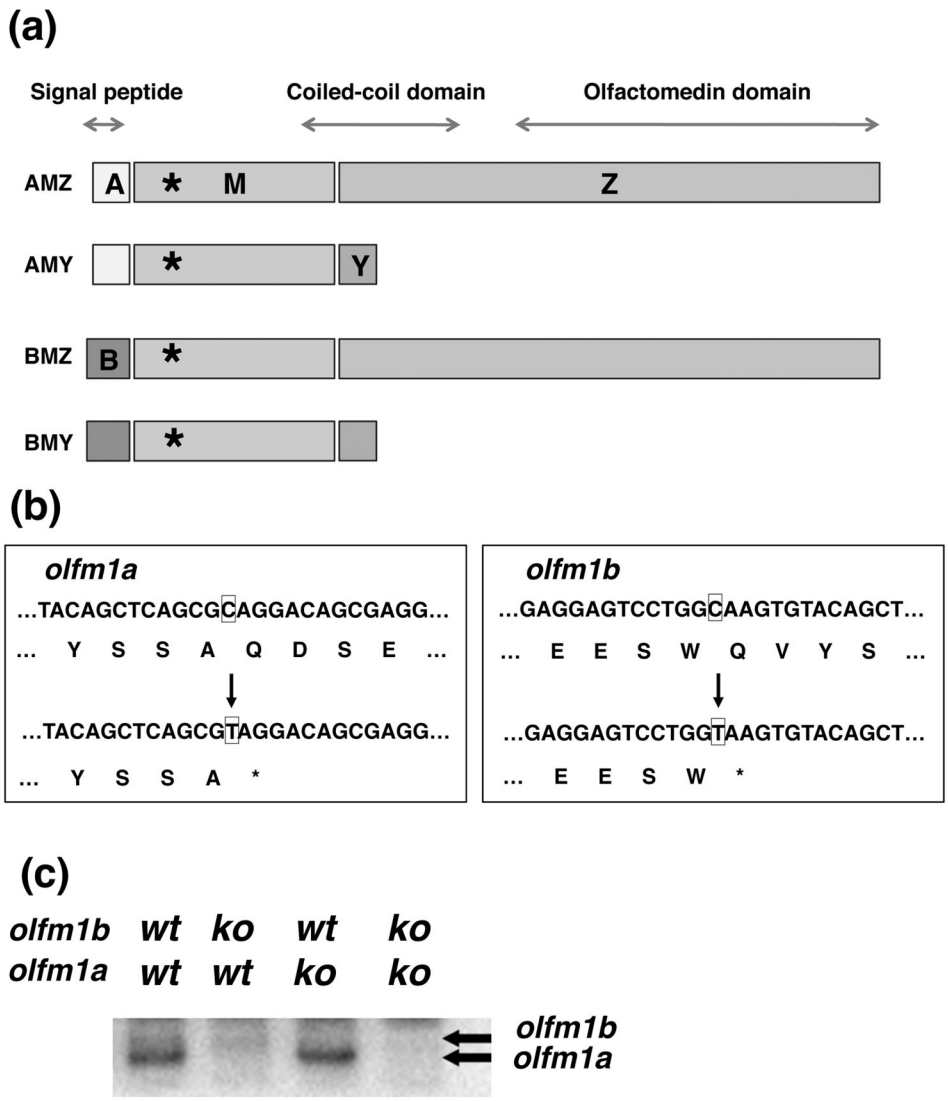

Fig. 1.

Generation of *olfm1* zebrafish null mutant. (a) Schematic diagram of olfm1 protein isoforms (AMZ, AMY, BMZ and BMY). The A or B regions contain a signal peptide, the M region is common between different olfm1 isoforms, and the Z region contains the olfactomedin domain. *Asterisks* mark positions of C-terminus in mutant proteins. (b) *Black arrows* indicate positions of nucleotide substitution in *olfm1a* and *olfm1b* sequences resulting in stop codons. The elimination of all naturally occurring isoforms of olfm1 proteins is produced by these nonsense mutations. (c) Western blot analysis of adult zebrafish brain from wt, *olfm1a*, *olfm1b* and *olfm1* null mutants using olfm1 antibodies. Positions of olfm1a and olfm1b proteins are shown by *arrows*. No olfm1 proteins were detected in *olfm1* null brain.

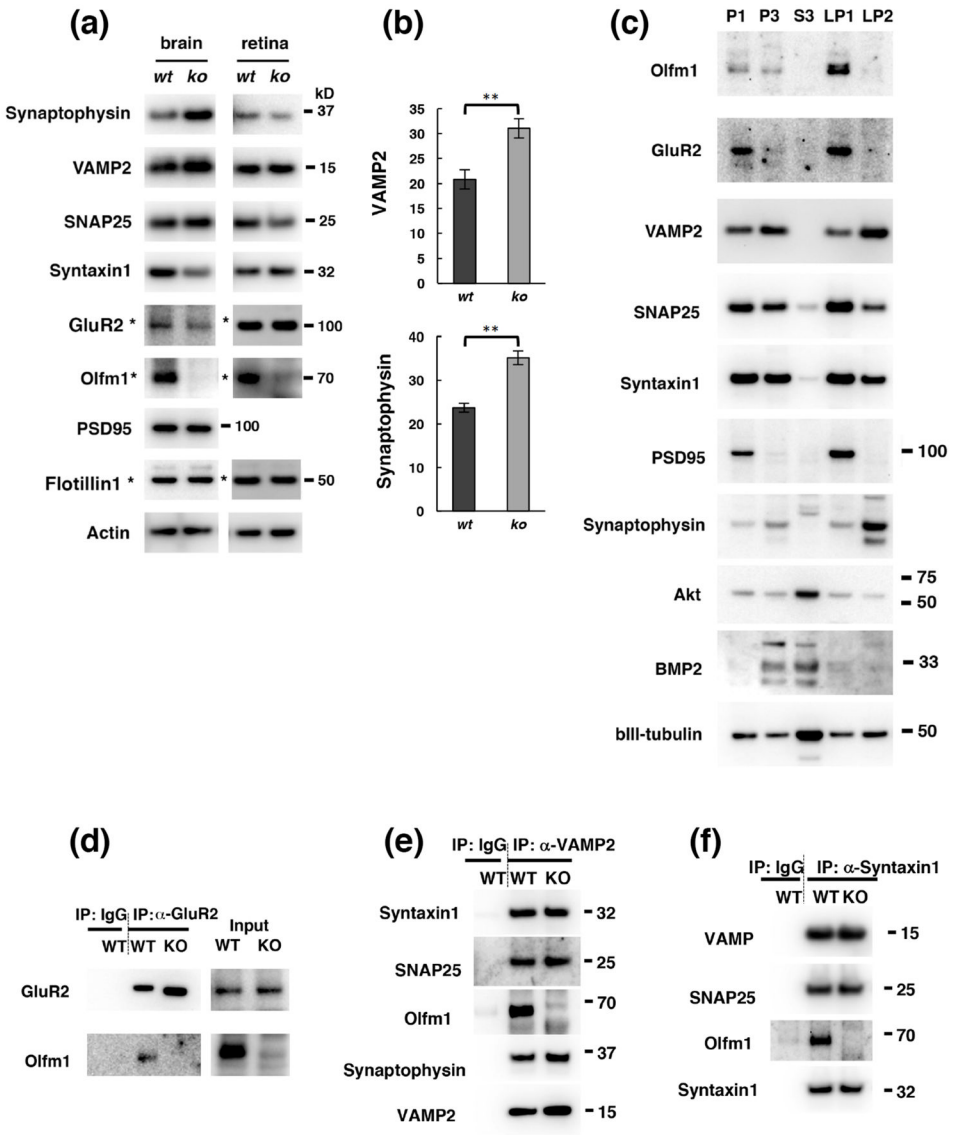

Fig. 2.

Olfm1 interacts with presynaptic SNARE complex proteins and postsynaptic GluR2 in synaptosomes from adult wt brain. (a) Western blot analysis of indicated proteins in adult wt and *olfm1* null zebrafish brain and retina. The blots marked by an *asterisk* was obtained in the P2 fraction. (b) Quantification of three independent experiments as in ***A*** for VAMP and synaptophysin. Data for each protein were normalized using beta-III tubulin level. **p < 0.01. (c) Biochemical fractionation of adult zebrafish brain and intracellular localization of olfm1 and some pre- and post-synaptic proteins in adult zebrafish brain. Note co-purification of olfm1 and several synaptosomal membrane proteins with the LP1 fraction but not with the soluble fraction (S3). (d) Co-immunoprecipitation of Olfm1 with GluR2 from the synaptosomal fraction. The levels of GluR2 and phosphorylated GluR2 were slightly increased in synaptosomes isolated from *olfm1* null brain compared with wt brain. (e, f) Co-immunoprecipitation of Olfm1 with VAMP2 and syntaxin1 from brain synaptosomes.

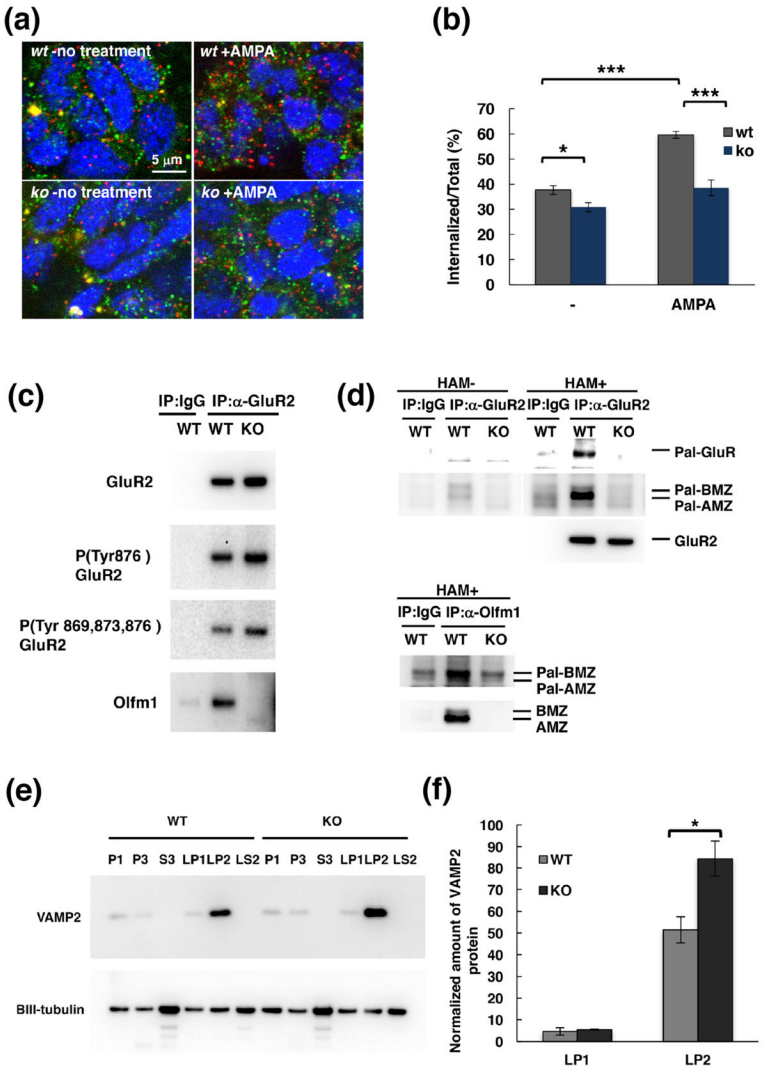

Fig. 3.

Changes in the localization of GluR2 and VAMP2 in *olfm1* null retina and brain. (a) The internalization of GluR2 in *olfm1* null and wt larval retinal cells in culture. Retina from 32 hpf larvae were dissected and cultured *in vitro* for 5 days. External GluR2s were labeled with antibodies against the N-terminal part of GluR2 and allowed to be internalized for 15 min with or without 100 μM AMPA in the culture. The external GluR2 was detected using Alexa488-secondary antibody. The internalized GluR2 was detected using Alexa555-secondary antibody after permeabilization of the cell membrane. Scale bar, 5 μm. (b) The number of green and red puncta was counted and the ratio of the internal and the total labeled GluR2 was calculated. $N = 6–8$ individual cultures. (c) The levels of GluR2 and phosphorylated GluR2 were slightly increased in synaptosomes isolated from *olfm1* null brain compared with wt brain. (d) Reduced palmitoylation of GluR2 precipitated by anti-GluR2 antibody from synaptosomes isolated from *olfm1* null brain compared with wt samples (upper panel). Note that olfm1 co-immunoprecipitated with GluR2 was also palmitoylated, indicating that olfm1 may be associated with membranes through its lipid

modification as well as its binding to other membrane-associated proteins (lower panel). HAM-untreated precipitates were used as a negative control and they show only weak signals for both GluR2 and Olfm1 (e) The level of VAMP2 was increased only in the synaptosomal LP2 fraction (synaptic vesicles) but not in LP2 (synaptosomal membrane). (f) Quantification of three independent experiments as in (f). *p<0.05,***< 0.001.

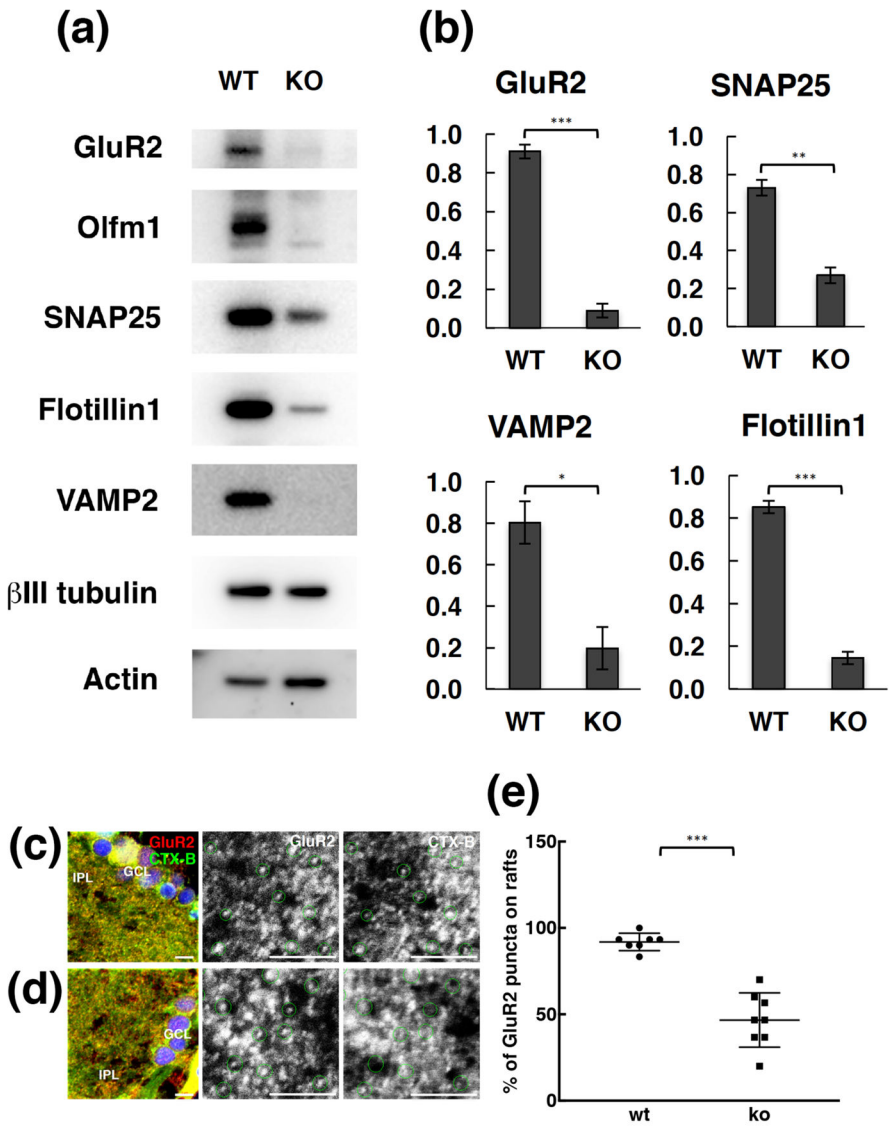

Fig. 4.

Characterization of the microdomain fraction from wt and *olfm1* null brain. (a) Changes in the protein levels detected in the microdomain fraction from wt and *olfm1* null adult brain. (b) Quantification of the results of three independent experiments as in (a). (c, d) GluR2 localization in CTX-B-labeled lipid rafts in the IPL of adult *wt* (c) and *olfm1* null (d) zebrafish retina. The black/white images in the middle and right rows represent enlarged images in each channel from the red squared areas in the left row. Note that all green circled GluR2-positive puncta are localized in CTX-B bound lipid rafts in wt retina, while some of GluR2 puncta in *olfm1* null are not in lipid rafts. Scale bar, 5 μm. (**e**) Quantification of the results of seven wt and eight *olfm1* null independent eye sections as in (c and d). *p<0.05, **p< 0.01, ***p< 0.001.

Table 1

Antibodies used in the study.

Antibody to	host	Company	Cat#	Resource Identifier	Used for (Work Dilution)
Actin	goat	Santa Cruz	sc-1616	RRID:AB_630836	WB (1:1,000)
βIII tubulin	chicken	Abcam	ab41489	RRID:AB_727049	WB (1:30,000)
Flotillin1	mouse	BD Transduction Lab.	610820	RRID:AB_398139	WB (1:250)
Synaptophysin	mouse	Synaptic Systems	101011	RRID:AB_887824	WB (1:10,000)
Syntaxin1	mouse	Synaptic Systems	110011	RRID:AB_887844	WB (1:10,000), IP
PSD95	mouse	Thermo Fisher Sci.	MA1-046	RRID:AB_2092361	WB (1:2000)
SNAP25	mouse	Synaptic Systems	111011	RRID:AB_887794	WB (1:1,000), IF (1:400)
GFP	chicken	Aves	GFP-1020	RRID:AB_10000240	IF (1:500)
GluR2	mouse	Millipore	MAB397	RRID:AB_2113875	WB (1:2,000), IF (1:500)
GluR2	mouse	Millipore	MABN71	RRID:AB_10806492	IF (1:500), IP
GluR2 P(Tyr876)	rabbit	Cell Signaling Tech.	#4027	RRID:AB_1147622	WB (1:1,000)
GluR2 P(Tyr 869,873,876)	rabbit	Cell Signaling Tech.	#3921	RRID:AB_1642146	WB (1:1,000)
zpr1	mouse	DSHB	zpr-1	RRID:AB_10013803	IF (1:200)
VAMP2	rabbit	Abcam	ab70222	RRID:AB_1271445	WB (1:3,000)
Islet1	mouse	DSHB	40.2D6 and 39.4D5		IF (1:250 each and mix)
PKCβ1	rabbit	Santa Cruz	sc-209	RRID:AB_2168968	IF (1:300)
Olfm1	rabbit	Covance	custom		IF (1:100), IP
Akt	rabbit	Cell Signaling Tech.	#9272	RRID:AB_329827	WB (1:1,000)
BMP2	goat	Santa Cruz	sc-6895	RRID:AB_2063364	WB (1:1,000)